

ELECTRONIC SUPPLEMENTARY INFORMATION

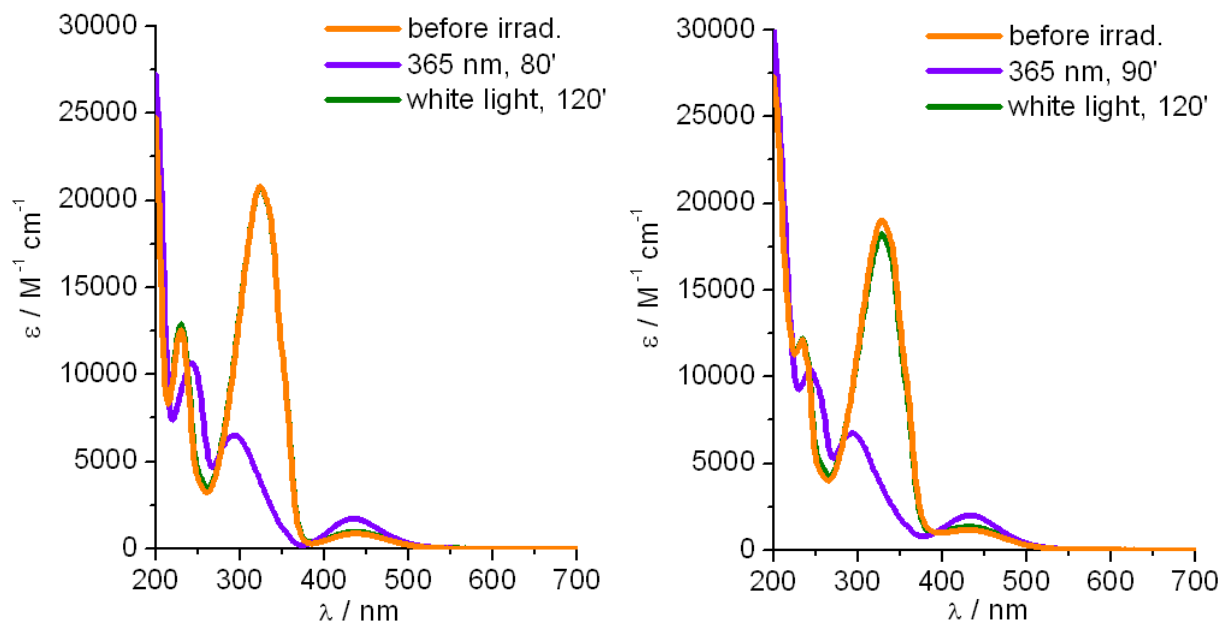


Fig. SI-1. (Left) UV/Vis spectra of H_3azo in methanol, showing reversible photoisomerization (concentration $7.1 \cdot 10^{-4}$ M, cell path 0.1 mm). (Right) UV/Vis spectra of H_3azoMe_2 in methanol, showing reversible photoisomerization (concentration $6.7 \cdot 10^{-4}$ M, cell path 0.1 mm).

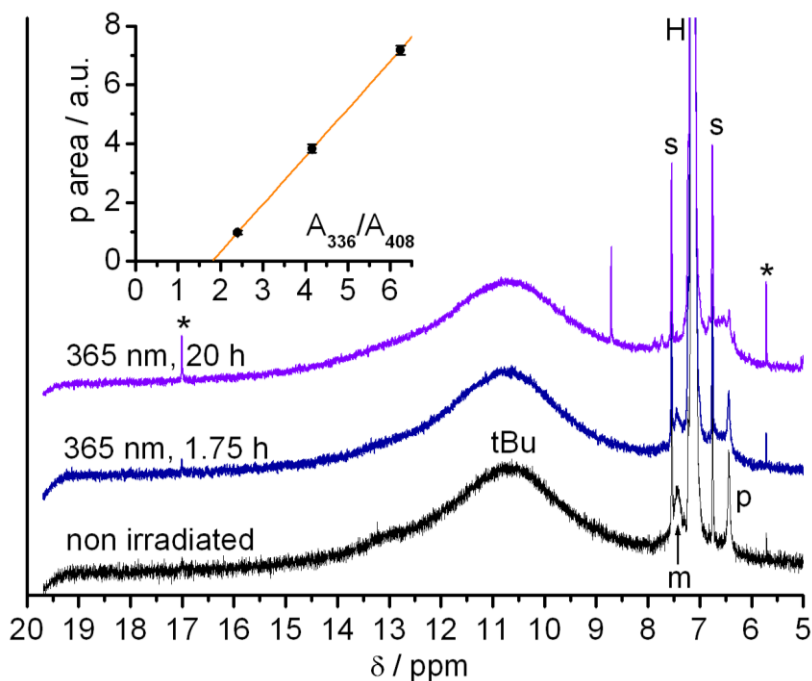


Fig. SI-2. ^1H NMR spectra of $\text{Fe}_4\text{azoMe}_2$ in benzene- d_6 (4.2 mg in 0.91 mL, 2.4 mM) before irradiation and after two different treatments with 365-nm light (benzene was preferred to toluene to minimize the number of signals from protio impurities). The broad peak around 10.6 ppm is characteristic of *tert*-butyl groups of dpm^- ligands (Ref. 3a). The narrow peaks are due to protio impurities in the solvent (H = main peak; s = satellites) and to traces of free

Hdpm (*). Since a phenyl substituent on the tripodal ligand gives no detectable NMR signal in the aromatic region due to extensive paramagnetic shift and broadening, the peaks labelled as *m* and *p* are assigned to the meta and para hydrogens of the 3,5-dimethylphenyl substituent. Upon irradiation, their intensity progressively decreases and a very broad peak appears around 6.6 ppm. Immediately after recording the NMR spectrum a portion of the solution was rapidly diluted in anhydrous benzene and its electronic spectrum recorded (the whole procedure lasted no more than 20', during which time the samples were handled in the dark). Since solution spectra in Fig. 1 (right) exhibit an isosbestic point at 408 nm, the absorbance at this wavelength was used to normalize the spectra. The inset of Fig. SI-2 shows that the normalized absorbance at 336 nm varies linearly with the area of the *p* peak. The calibration curve so obtained has been used to relate the absorbance at the maximum (336-340 nm) to the fraction of *trans* ligand isomer in solution and in polymer matrices. To this aim, it was assumed that the non-irradiated solution of Fig. SI-2 features 100% *trans* azo ligands.

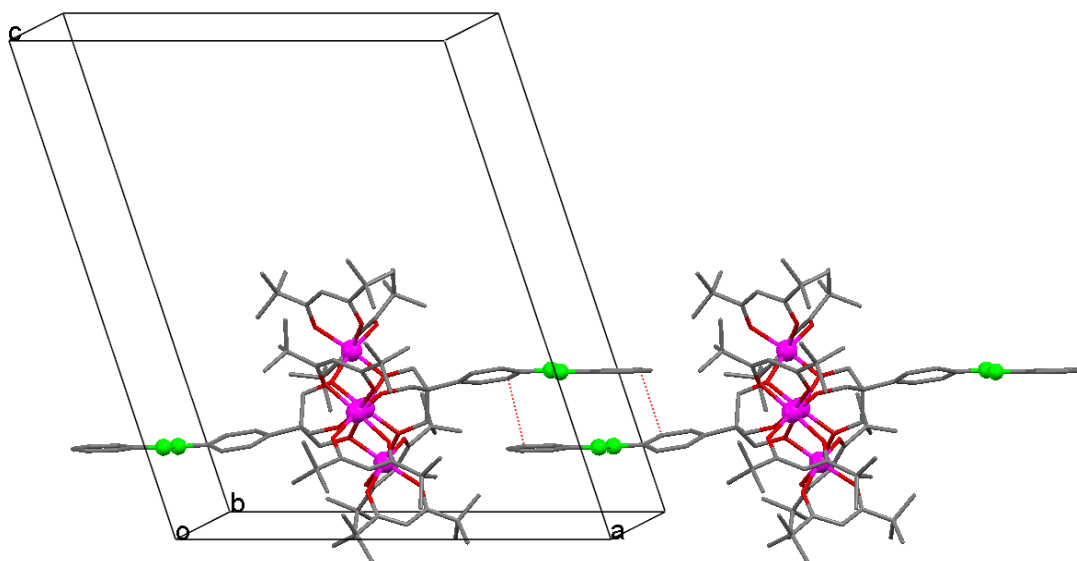


Fig. SI-3. Interaction of neighboring molecules in the crystal structure of **Fe₄azo** to give chains developing along the **a** axis.

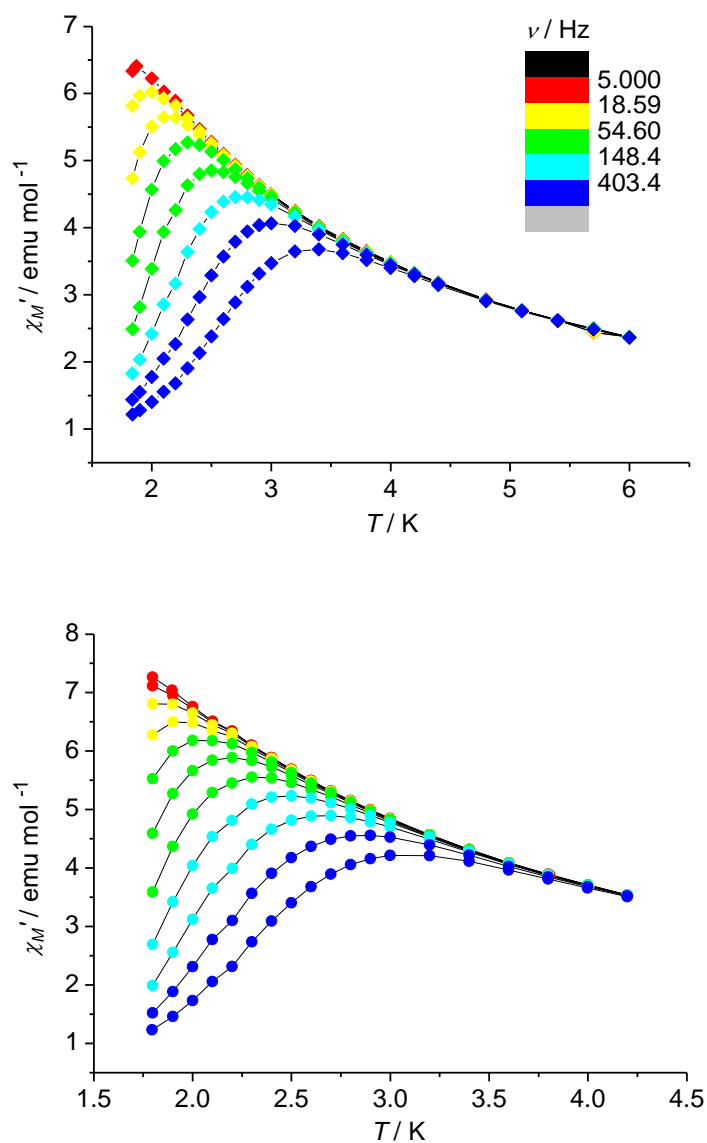


Fig. SI-4. Temperature dependence of the in-phase molar magnetic susceptibility (χ_M') of Fe_4azo (*top*) and $\text{Fe}_4\text{azoMe}_2$ (*bottom*), measured for 8 and 11 logarithmically spaced frequencies, respectively, in the 10 – 1000 Hz range with a 1 kOe static applied field. Lines are a guide to the eye.

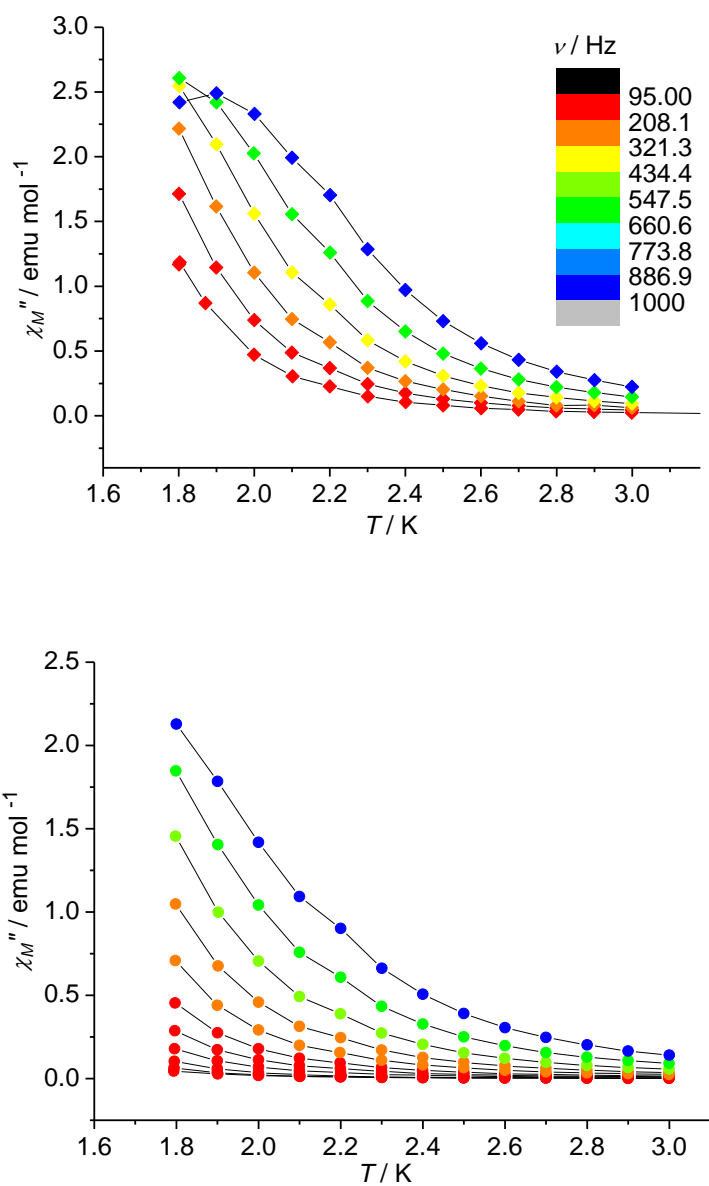


Fig. SI-5. Temperature dependence of the out-of-phase molar magnetic susceptibility (χ_M'') of Fe_4azo (*top*) and $\text{Fe}_4\text{azoMe}_2$ (*bottom*), measured for logarithmically spaced frequencies in the 10 – 1000 Hz range in zero static applied field. Lines are a guide to the eye.

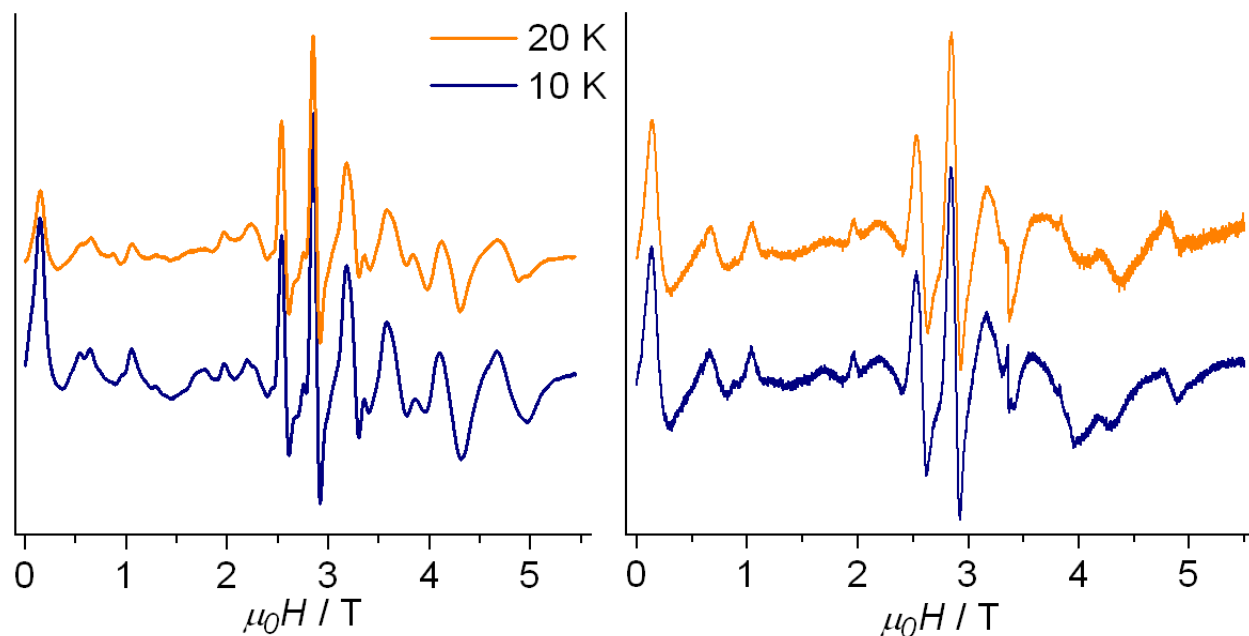


Fig. SI-6. W-band EPR spectra of powder samples of Fe_4azo (left) and $\text{Fe}_4\text{azoMe}_2$ (right) at two temperatures.

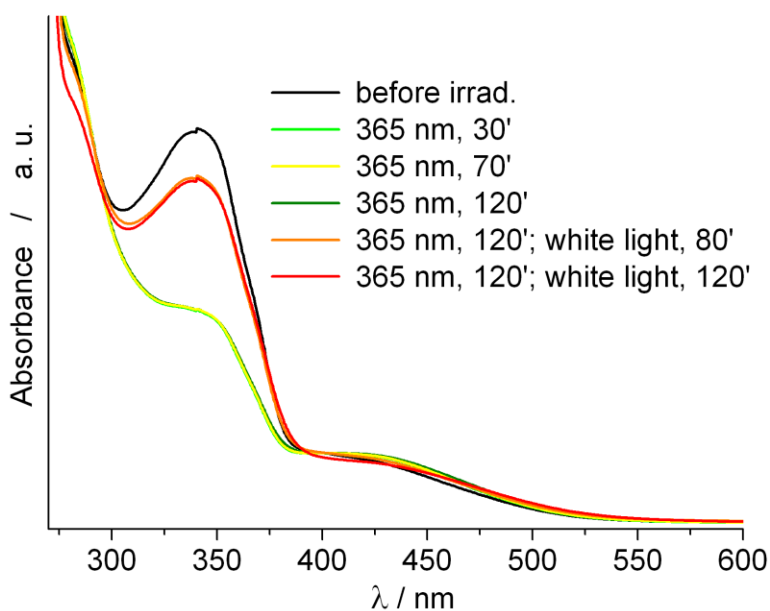


Fig. SI-7. UV/Vis spectra of $\text{Fe}_4\text{azoMe}_2$ dispersed in polystyrene (4 % w/w) for different irradiation conditions, showing the retention of photochemical activity of the diazo moieties and the achievement of photostationary states.

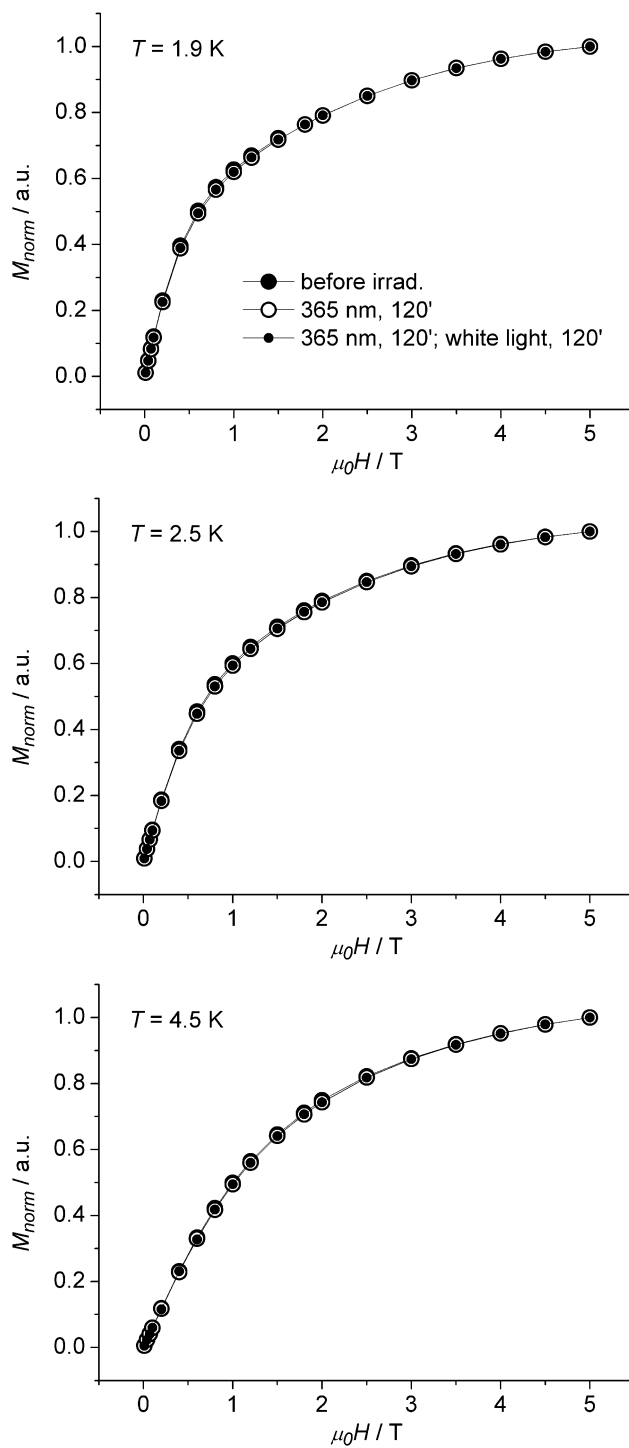


Fig. SI-8. Field dependence of the magnetization of $\text{Fe}_4\text{azoMe}_2$ dispersed in polystyrene (4 % w/w) for different irradiation conditions. Data are normalized to the magnetization value measured at the highest field (50 kOe). Lines are a guide to the eye.

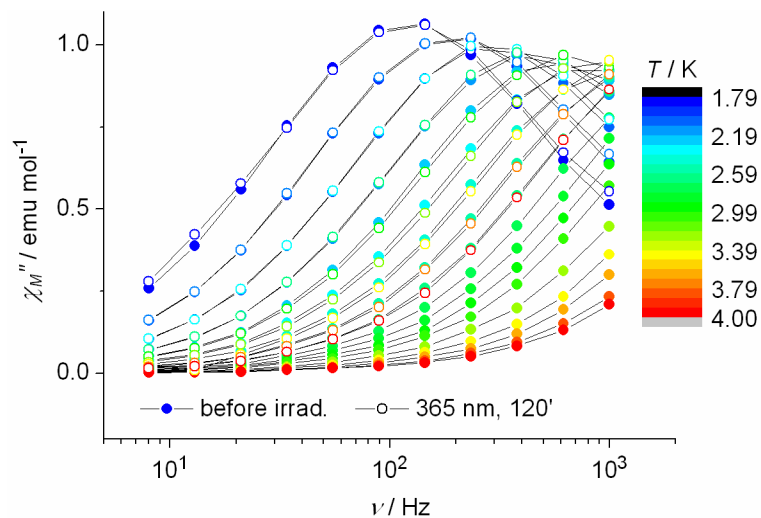


Fig. SI-9. Frequency dependence of the out-of-phase molar magnetic susceptibility (χ_M'') of **Fe₄azoMe₂** dispersed in polystyrene (4 % w/w). The behaviour before and after UV irradiation has been probed at 11 logarithmically-spaced frequency values in the range 10 – 1000 Hz, with a static applied field of 1 kOe. Lines are a guide to the eye.